

## New $\mu_4$ -Oxido-Bridged Copper Benzoate Quasi-Tetrahedron and Bis- $\mu_3$ -Hydroxido-Bridged Copper Azide and Copper Thiocyanate Stepped Cubanes: Core Conversion, Structural Diversity, and Magnetic Properties

Mrinal Sarkar,<sup>†</sup> Rodolphe Clérac,<sup>‡,◇</sup> Corine Mathonière,<sup>§</sup> Nigel G. R. Hearns,<sup>‡,◇</sup> Valerio Bertolasi,<sup>⊥</sup> and Debashis Ray<sup>\*,†</sup>

<sup>†</sup>Department of Chemistry, Indian Institute of Technology, Kharagpur 721 302, India, <sup>‡</sup>CNRS, UPR 8641, Centre de Recherche Paul Pascal (CRPP), Equipe “Matériaux Moléculaires Magnétiques”, 115 Avenue du Dr. Albert Schweitzer, Pessac, F-33600, France, <sup>◇</sup>Université de Bordeaux, UPR 8641, Pessac, F-33600, France, <sup>§</sup>Institut de Chimie de la Matière Condensée de Bordeaux (ICMCB), CNRS, Université de Bordeaux, 87 Avenue du Dr. Albert Schweitzer, Pessac Cedex, F-33608, France, and <sup>⊥</sup>Dipartimento di Chimica e Centro di Strutturistica Diffraattometrica, Università di Ferrara, Via Borsari 46, 44100 Ferrara, Italy

Received February 22, 2010

[Cu<sub>2</sub>( $\mu_4$ -O)Cu<sub>2</sub>] and [Cu<sub>2</sub>( $\mu_3$ -OH)<sub>2</sub>Cu<sub>2</sub>] geometrical arrangements are found in a new family of tetranuclear complexes: [Cu<sub>4</sub>( $\mu_4$ -O)( $\mu$ -bip)<sub>2</sub>( $\mu$ -O<sub>2</sub>CPh)<sub>4</sub>]·0.5CH<sub>2</sub>Cl<sub>2</sub> (1·0.5CH<sub>2</sub>Cl<sub>2</sub>), [Cu<sub>4</sub>( $\mu_3$ -OH)<sub>2</sub>( $\mu$ -bip)<sub>2</sub>(N<sub>3</sub>)<sub>4</sub>] (2), and [Cu<sub>4</sub>( $\mu_3$ -OH)<sub>2</sub>( $\mu$ -bip)<sub>2</sub>(NCS)<sub>4</sub>(DMF)<sub>2</sub>] (3·2DMF) [Hbip = 2,6-bis(benzyliminomethyl)-4-methylphenol; DMF = dimethylformamide]. These complexes have been characterized by X-ray crystallography, and their magnetic properties have been studied. Complex 1 reacts with azide and thiocyanate anions, leading to 2 and 3 with a change of the [Cu<sub>4</sub>( $\mu_4$ -O)] core into [Cu<sub>4</sub>( $\mu_3$ -OH)<sub>2</sub>] units. These compounds are new examples of [Cu<sub>4</sub>] complexes where Cu<sup>II</sup> ions are connected by two types of water-derived ligands: oxide and hydroxide. Formation of these [Cu<sub>4</sub>] complexes can be controlled by changing the bridging ligands, which allows an effective tuning of the self-assembly. The study of the magnetic properties reveals that these complexes exhibit strong intramolecular antiferromagnetic interactions to yield a S<sub>T</sub> = 0 ground state. For the three complexes, the temperature dependence of the magnetic susceptibility was fitted using a model with two isolated S = 1/2 dimers based on the  $H = -2J\{S_{Cu,1} \cdot S_{Cu,2}\}$  spin Hamiltonian with  $J/k_B = -289$  K for 1;  $J/k_B = -464$  and  $-405$  K for 2 and 3, respectively (where  $J$  is the exchange constant through the oxido–phenoxido or hydroxido–phenoxido bridges, respectively).

### Introduction

The synthetic coordination chemistry based on controlled aggregation via self-assembly of small building units to form polynuclear complexes is of contemporary interest. The role of ligand design and fine-tuning of reaction conditions with co-ligands are crucial to understand and control the aggregation process. Progresses in understanding the aggregation reactions are likely to be developed by studying the self-assembly processes of simple building units such as [Cu<sub>2</sub>]/ligand units in the presence of other secondary nucleating groups. [Cu<sub>2</sub>] complexes have often been used as models to study the magnetic-exchange interactions,<sup>1–3</sup> DNA binding

and cleavage,<sup>4</sup> and oxidation of catechols<sup>2,5,6</sup> and as building units for the construction of tetra- and polynuclear complexes with interesting magnetic properties.<sup>7–12</sup> Following this strategy, our research activity has focused on the design of new families of molecular aggregates based on [Cu<sub>2</sub>] building blocks. The tendency of the copper ions to receive a fifth coordination group at the apical binding site and the ability of the phenoxide ligands to bridge metal ions allow for

\*To whom correspondence should be addressed. Fax: 91-3222-82252. Tel: 03222-283324. E-mail: dray@chem.iitkgp.ernet.in.

(1) Paital, A. R.; Wu, A.-Q.; Guo, G.-C.; Aromí, G.; Ribas-Ariño, J.; Ray, D. *Inorg. Chem.* **2007**, *46*, 2947–2949.

(2) Banerjee, A.; Sarkar, S.; Chopra, D.; Colacio, E.; Rajak, K. K. *Inorg. Chem.* **2008**, *47*, 4023–4031.

(3) Paital, A. R.; Mitra, T.; Ray, D.; Wong, W. T.; Ribas-Ariño, J.; Novoa, J. J.; Ribasa, J.; Aromí, G. *Chem. Commun.* **2005**, 5172–5174.

(4) Lahiri, D.; Bhowmick, T.; Pathak, B.; Shameema, O.; Patra, A. K.; Ramakumar, S.; Chakravarty, A. R. *Inorg. Chem.* **2009**, *48*, 339–349.

(5) Nanda, P. K.; Bertolasi, V.; Aromí, G.; Ray, D. *Polyhedron* **2009**, *28*, 987–993.

(6) Banu, K. S.; Chattopadhyay, T.; Banerjee, A.; Bhattacharya, S.; Suresh, E.; Nethaji, M.; Zangrando, E.; Das, D. *Inorg. Chem.* **2008**, *47*, 7083–7093.

(7) Paital, A. R.; Mandal, D.; Huang, X.; Li, J.; Aromí, G.; Ray, D. *Dalton Trans.* **2009**, 1352–1362.

(8) Paital, A. R.; Bertolasi, V.; Aromí, G.; Ribas-Ariño, J.; Ray, D. *Dalton Trans.* **2008**, 861–864.

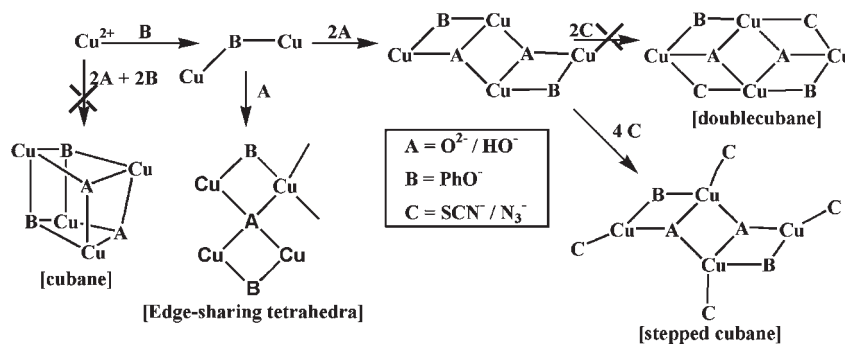
(9) Paital, A. R.; Hong, C. S.; Kim, H. C.; Ray, D. *Eur. J. Inorg. Chem.* **2007**, 1644–1653.

(10) Nanda, P. K.; Aromí, G.; Ray, D. *Chem. Commun.* **2006**, 3181–3183.

(11) Paital, A. R.; Nanda, P. K.; Das, S.; Aromí, G.; Ray, D. *Inorg. Chem.* **2006**, *45*, 505–507.

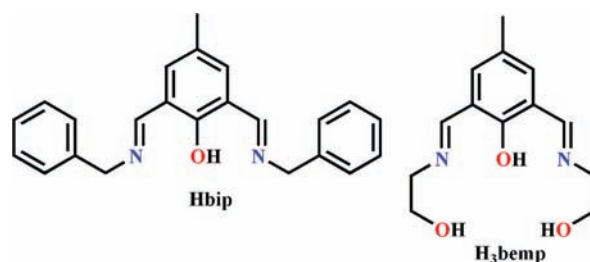
(12) Nanda, P. K.; Aromí, G.; Ray, D. *Inorg. Chem.* **2006**, *45*, 3143–3145.

**Scheme 1.** Utilization of One  $\mu_4$ -A ( $O^{2-}$ ) and Two  $\mu$ -B Bridges Provides a Tetrahedral  $[Cu_4]$  Assembly, Whereas Participation of Two  $\mu_3$ -A ( $HO^-$ ), Two  $\mu$ -B, and Four Terminal C Units Provides a Stepped Cubane  $[Cu_4]$  Assembly



the possibility of associating dinuclear Cu(II) units into discrete oligonuclear and polynuclear complexes. Depending on the number and nature of secondary bridging or coordinating groups, the assembly of two dinuclear units leads to four types of  $[Cu_4]$  aggregates: the tetrahedron, the cubane, the fused defective dicubane, and the stepped cubane (Scheme 1). Among these different geometries, tetrahedral and stepped cubane structures appear much less frequently.<sup>13–16</sup> We have been engaged in studying  $[Cu_4]$  complexes for some time because of their interest in bioinorganic modeling, multi-electron transfer, industrial and biological catalysis, and magnetostructural research.<sup>7–12,16</sup> Water and water-derived ligands such as hydroxido and oxido groups are most suitable bridging ligands in the construction and/or stabilization of  $[Cu_2]$  moieties and more generally in coordination chemistry.<sup>5,11,16,19–22</sup>  $\mu_4$ -Oxidotetracopper(II) cores,  $[Cu_4(\mu_4-O)]$ , are important both in industrial catalysis of converting substituted phenols to quinones<sup>17</sup> and in the biological catalytic cycle of nitrous oxide reduction to dinitrogen.<sup>18</sup> Recently, during oxidation of 2,3,6-trimethylphenol (TMP) with  $O_2$  to trimethyl quinone (TMQ), a key intermediate of vitamin E, in the presence of a catalytic amount of copper(II) chloride in ionic liquids a hexa- $\mu$ -chlorido-tetrachlorido- $\mu_4$ -oxidocuprate ( $4^-$ ) species  $[Cu_4(\mu_4-O)Cl_{10}]^{4-}$  was isolated as an active species.<sup>17</sup> In trying to isolate and study new forms of such aggregates, we have been interested in exploring the reactivity of the tetradentate/dinucleating phenolate Schiff base ligand Hbip (Chart 1, left; 2,6-bis(benzyliminomethyl)-4-

**Chart 1.** Ligands



methylphenol)<sup>23</sup> with  $Cu^{II}$  metal ions in the presence of additional ligands such as  $PhCO_2^-$ ,  $N_3^-$ , and  $NCS^-$ . The use of  $H_3bemp$  (Chart 1, right, 2,6-bis(2-hydroxyethyliminomethyl)-4-methylphenol), a closely related ligand to Hbip, leads to interesting systems, consisting of  $[Co_4]$ ,<sup>24</sup>  $[Ni_6]$ ,<sup>25</sup> and  $[Cu_{18}]$ <sup>26</sup> complexes and a large heterometallic  $[Mn_6Cu_{10}]$ <sup>27</sup> species. Herein, two classes of stable  $[Cu_4]/bip^-$  complexes are reported: (i)  $[Cu_4(\mu_4-O)(\mu-bip)_2(\mu-O_2CPh)_4]$  (**1**), which contains a central tetrahedral  $\mu_4$ -oxido coordinating group, and (ii)  $[Cu_4(\mu_3-OH)_2(\mu-bip)_2(N_3)_4]$  (**2**) and  $[Cu_4(\mu_3-OH)_2(\mu-bip)_2(NCS)_4(DMF)_2]$  (**3**), obtained by converting **1** and its  $\mu_4$ -oxido group into stepped cubane complexes with bis-OH bridges. These complexes have been isolated and crystallographically characterized, and their magnetic properties have been studied.

## Experimental Section

**Materials.** The chemicals used were obtained from the following sources: Copper acetate monohydrate, ammonium thiocyanate, sodium azide, and benzylamine from SRL (India) and sodium benzoate from S.D. Fine Chemicals (India). All other chemicals and solvents were reagent grade materials and were used as received without further purification.

**Syntheses. Hbip Ligand.** The Hbip Schiff base is prepared from the single-step condensation of 2,6-diformyl-5-methylphenol (1.640 g, 10 mmol) and benzylamine (2.18 mL, 20 mmol) in methanol (40 mL) under reflux for 1 h, as reported previously.<sup>23</sup>

$[Cu_4(\mu_4-O)(\mu-bip)_2(\mu_{1,3}-O_2CPh)_4] \cdot 0.5CH_2Cl_2$  (**1**· $0.5CH_2Cl_2$ ). To the yellow MeOH solution (25 mL) of Hbip (0.342 g, 1.00 mmol) is added  $Cu(OAc)_2 \cdot H_2O$  (0.400 g, 2.00 mmol) with stirring at ambient temperature in air. The brown solution formed initially changes to green in about 5 min. The resulting green solution is

(24) Mandal, D.; Ray, D. *Inorg. Chem. Commun.* **2007**, *10*, 1202–1205.

(25) Mandal, D.; Bertolasi, V.; Ribas-Ariño, J.; Aromí, G.; Ray, D. *Inorg. Chem.* **2008**, *47*, 3465–3467.

(26) Shiga, T.; Maruyama, K.; Han, L. Q.; Oshio, H. *Chem. Lett.* **2005**, *34*, 1648–1649.

(27) Yamashita, S.; Shiga, T.; Kurashina, M.; Nihei, M.; Nojiri, H.; Sawa, H.; Kakiuchi, T.; Oshio, H. *Inorg. Chem.* **2007**, *46*, 3810–3812.

(13) Shakyia, R.; Keyes, P. H.; Heeg, M. J.; Moussawel, A.; Heiney, P. A.; Verani, C. N. *Inorg. Chem.* **2006**, *45*, 7587–7589.

(14) Kirillov, A. M.; Kopylovich, M. N.; Kirillova, M. V.; Haukka, M.; Silva, M. F. C. G. da; Pombeiro, A. J. L. *Angew. Chem., Int. Ed.* **2005**, *44*, 4345–4349.

(15) Isele, K.; Franz, P.; Ambrus, C.; Bernardinelli, G.; Decurtins, S.; Williams, A. F. *Inorg. Chem.* **2005**, *44*, 3896–3906.

(16) Bera, M.; Wong, W. T.; Aromí, G.; Ribas, J.; Ray, D. *Inorg. Chem.* **2004**, *43*, 4787–4789.

(17) Sun, H.; Harms, K.; Sundermeyer, J. J. *Am. Chem. Soc.* **2004**, *126*, 9550–9551.

(18) Prudêncio, M.; Pereira, A. S.; Tavares, P.; Besson, S.; Cabrito, I.; Brown, K.; Samyn, B.; Devreese, B.; Beumen, J. V.; Rusnak, F.; Fauque, G.; Moura, J. J. G.; Tegoni, M.; Cambillau, C.; Moura, I. *Biochemistry* **2000**, *39*, 3899–3907.

(19) Paul, S.; Clérac, R.; Hearn, N. G. R.; Ray, D. *Cryst. Growth Des.* **2009**, *9*, 4032–4040.

(20) Mukherjee, A.; Rudra, I.; Nethaji, M.; Ramasesha, S.; Chakravarty, A. R. *Inorg. Chem.* **2003**, *42*, 463–468.

(21) Dhara, K.; Ratha, J.; Manassero, M.; Wang, X.-Y.; Gao, S.; Banerjee, P. J. *Inorg. Biochem.* **2007**, *101*, 95–103.

(22) Pradeep, C. P.; Supriya, S.; Zacharias, P. S.; Das, S. K. *Polyhedron* **2006**, *25*, 3588–3592.

(23) Grzybowski, J. J.; Urbach, F. L. *Inorg. Chem.* **1980**, *19*, 2604–2608.

stirred for ca. 10 min, and  $\text{NaO}_2\text{CPh}$  (0.288 g, 2.0 mmol) is added. The green suspensions formed initially change to green solution in about 15 min, and after 1 h, a green precipitate appears. The green solid is isolated by filtration, washed with cold methanol, and dried under vacuum over  $\text{P}_4\text{O}_{10}$ . The green prismatic-shaped single crystals suitable for X-ray analysis are obtained from a  $\text{CH}_2\text{Cl}_2$ –MeOH solvent mixture after 5 days. Yield: 0.524 g, 73%. Anal. Calcd for  $\text{C}_{74.5}\text{H}_{63}\text{Cu}_4\text{N}_4\text{O}_{11}\text{Cl}$  (1479.97 g mol<sup>-1</sup>): C, 60.46; H, 4.29; N, 3.78. Found: C, 60.38; H, 4.18; N, 3.58. Selected FTIR bands (KBr, cm<sup>-1</sup>; s = strong, vs = very strong, m = medium, br = broad): 1623 (s), 1609 (s), 1568 (s), 1455 (s), 1371 (s), 1234 (m), 760 (m), 718 (s), 679 (s), 623 (m), 494 (m). Molar conductance,  $\Lambda_M$  ( $\text{CH}_2\text{Cl}_2$  solution): 3  $\Omega^{-1}\text{cm}^2\text{mol}^{-1}$ . UV–vis spectra [ $\lambda_{\text{max}}$ , nm ( $\epsilon$ , L mol<sup>-1</sup> cm<sup>-1</sup>)]: ( $\text{CH}_2\text{Cl}_2$  solution) 680 (210), 389 (4895), 326 (3534), 253 (21695).

**[Cu<sup>II</sup><sub>4</sub>( $\mu_3$ -OH)<sub>2</sub>( $\mu$ -bip)<sub>2</sub>(N<sub>3</sub>)<sub>4</sub>] (2). Method A via Direct Route.**  $\text{Cu}(\text{OAc})_2 \cdot \text{H}_2\text{O}$  (0.20 g, 1.00 mmol) dissolved in methanol (25 mL) is added dropwise with stirring to a yellow MeOH solution (15 mL) of Hbip (0.171 g, 0.50 mmol). The brown solution formed initially changes to green after about 5 min of stirring. After ca. 10 min a solution of  $\text{NaN}_3$  (0.130 g, 2.0 mmol) in MeOH (25 mL) is added dropwise. The color of the reaction mixture changes to dark green, and the reaction mixture is stirred further for about 30 min. The obtained green precipitate is collected by filtration, washed with cold methanol followed by water, and dried under vacuum over  $\text{P}_4\text{O}_{10}$ . Single crystals suitable for X-ray analysis are obtained from DMF after 7 days. Yield: 0.202 g, 71%. Anal. Calcd for  $\text{C}_{46}\text{H}_{42}\text{N}_{16}\text{O}_4\text{Cu}_4$  (1137.13 g mol<sup>-1</sup>): C, 48.58; H, 3.72; N, 19.70. Found: C, 48.50; H, 3.61; N, 19.44. Selected FTIR bands (KBr, cm<sup>-1</sup>): 3600 (br), 3448 (br) 2043 (vs), 1637 (vs), 1560 (vs), 1347 (s), 1092 (m), 829 (m), 755 (m), 711 (m). Molar conductance,  $\Lambda_M$  (DMF solution): 6  $\Omega^{-1}\text{cm}^2\text{mol}^{-1}$ . UV–vis spectra [ $\lambda_{\text{max}}$ , nm ( $\epsilon$ , L mol<sup>-1</sup> cm<sup>-1</sup>)]: (DMF solution): 655 (520), 378 (9480), 353 (4450), 274 (13 658).

**Method B via Conversion of 1.** A green solution of **1** (0.360 g, 0.25 mmol) in  $\text{CH}_2\text{Cl}_2$  (25 mL) is stirred for about 5 min followed by a dropwise addition of  $\text{NaN}_3$  (0.097 g, 1.50 mmol) dissolved in MeOH (20 mL) at ambient temperature. During the reaction, there is a noticeable color change from green to dark green followed by separation of a green precipitate, which is easily collected by filtration, washed with cold methanol, and dried under vacuum over  $\text{P}_4\text{O}_{10}$ . Yield: 0.180 g, 63%. Anal. Calcd for  $\text{C}_{46}\text{H}_{42}\text{N}_{16}\text{O}_4\text{Cu}_4$  (1137.13 g mol<sup>-1</sup>): C, 48.58; H, 3.72; N, 19.70. Found: C, 48.45; H, 3.63; N, 19.54. Selected FTIR bands (KBr, cm<sup>-1</sup>): 3601 (br), 3448 (br) 2045 (vs), 1638 (vs), 1558 (vs), 1350 (s), 1094 (m), 832 (m), 758 (m), 707 (m). Molar conductance,  $\Lambda_M$  (DMF solution): 8  $\Omega^{-1}\text{cm}^2\text{mol}^{-1}$ . UV–vis spectra [ $\lambda_{\text{max}}$ , nm ( $\epsilon$ , L mol<sup>-1</sup> cm<sup>-1</sup>)]: (DMF solution): 655 (525), 378 (9483), 353 (4452), 274 (13 655).

**Caution!!** Azide complexes of metal ions involving organic ligands are potentially explosive. Only small quantities of the complexes should be prepared, and these should be handled with care.

**[Cu<sup>II</sup><sub>4</sub>( $\mu_3$ -OH)<sub>2</sub>( $\mu$ -bip)<sub>2</sub>(NCS)<sub>4</sub>(DMF)<sub>2</sub>]·2DMF (3·2DMF). Method A via Direct Route.** The green compound **3** is obtained by a similar method to that described above for compound **2** by using  $\text{NH}_4\text{SCN}$  (0.152 g, 2.0 mmol) instead of  $\text{NaN}_3$ . The reaction in the presence of up to 6 mmol of  $\text{NH}_4\text{SCN}$  yields complex **3** exclusively. Yield: 0.210 g, 70%. Green single crystals of **3**·2DMF suitable for X-ray analysis are obtained from DMF during 7 days. Anal. Calcd for  $\text{C}_{62}\text{H}_{72}\text{N}_{12}\text{O}_8\text{S}_4\text{Cu}_4$  (1495.77 g mol<sup>-1</sup>): C, 49.78; H, 4.85; N, 11.24. Found: C, 49.70; H, 4.74; N, 11.02. Selected FTIR bands (KBr, cm<sup>-1</sup>): 3600 (br), 3433 (br), 2081 (vs), 1655 (vs), 1636 (vs), 1562 (s), 1451 (m), 1333 (m), 1092 (m), 829 (m), 760 (m), 709 (m). Molar conductance,  $\Lambda_M$  (DMF solution): 5  $\Omega^{-1}\text{cm}^2\text{mol}^{-1}$ . UV–vis spectra [ $\lambda_{\text{max}}$ , nm ( $\epsilon$ , L mol<sup>-1</sup> cm<sup>-1</sup>)]: (DMF solution): 665 (525), 378 (6820), 353 (4134), 274 (13 834).

**Method B via Conversion of 1.** Compound **3** is also obtained quantitatively following the conversion method used in the case of **2** by replacing  $\text{NaN}_3$  by  $\text{NH}_4\text{SCN}$ . The green precipitate is collected by filtration, washed with cold methanol, and dried under vacuum over  $\text{P}_4\text{O}_{10}$ . Yield: 0.180 g, 60%. Anal. Calcd for  $\text{C}_{62}\text{H}_{72}\text{N}_{12}\text{O}_8\text{S}_4\text{Cu}_4$  (1495.77 g mol<sup>-1</sup>): C, 49.78; H, 4.85; N,

11.24. Found: C, 49.68; H, 4.75; N, 11.09. Selected FTIR bands (KBr, cm<sup>-1</sup>): 3600 (br), 3435 (br), 2079 (vs), 1653 (vs), 1638 (vs), 1560 (s), 1450 (m), 1336 (m), 1090 (m), 829 (m), 758 (m), 713 (m). Molar conductance,  $\Lambda_M$  (DMF solution): 6  $\Omega^{-1}\text{cm}^2\text{mol}^{-1}$ . UV–vis spectra [ $\lambda_{\text{max}}$ , nm ( $\epsilon$ , L mol<sup>-1</sup> cm<sup>-1</sup>)]: (DMF solution): 665 (521), 378 (6823), 353 (4136), 274 (13 840).

**Physical Measurements.** The elemental analyses (C, H, N) were performed with a Perkin-Elmer model 240C elemental analyzer. FTIR spectra were recorded on a Perkin-Elmer 883 spectrometer. The solution electrical conductivity and electronic spectra were obtained using a Unitech type U131C digital conductivity meter with a solute concentration of about 10<sup>-3</sup> M and a Shimadzu UV 3100 UV–vis–NIR spectrophotometer, respectively. The powder X-ray diffraction (PXRD) patterns were obtained using a Phillips PW 1710 diffractometer with Cu K $\alpha$  radiation. The magnetic susceptibility measurements were obtained with the use of a Quantum Design SQUID magnetometer MPMS-XL housed at the Centre de Recherche Paul Pascal. This magnetometer works between 1.8 and 300 K for dc applied fields ranging from -7 to 7 T. Measurements were performed on polycrystalline samples of 13.70, 29.33, and 12.16 mg for **1**·0.5 $\text{CH}_2\text{Cl}_2$ , **2**, and **3**·2DMF, respectively. The magnetic data were corrected for the sample holder and the diamagnetic contributions.

**Crystal Data Collection and Refinement for 1·0.5 $\text{CH}_2\text{Cl}_2$ , 2, and 3·2DMF.** Crystal data of compound **1**·0.5 $\text{CH}_2\text{Cl}_2$  were collected on a Nonius Kappa CCD diffractometer using graphite-monochromated Mo K $\alpha$  radiation ( $\lambda = 0.7107 \text{ \AA}$ ) at low temperature (120 K). Data sets were integrated with the Denzo-SMN package<sup>28</sup> and corrected for Lorentz–polarization and absorption<sup>29</sup> effects. The structure was solved by direct methods (SIR97)<sup>30</sup> and refined by full-matrix least-squares methods with all non-hydrogen atoms anisotropic and hydrogens included on calculated positions, riding on their carrier atoms. The phenyl group C34/C39 was found disordered and was refined isotropically over two positions with occupancies of 0.6 and 0.4, respectively. The molecule of solvent,  $\text{CH}_2\text{Cl}_2$ , was found disordered around a center of symmetry and was refined over two positions with occupancy of 0.5 each. All calculations were performed using SHELXL-97<sup>31</sup> and PARST<sup>32</sup> implemented in the WINGX system of programs.<sup>33</sup> The crystal data of the complex **2** were collected on a Nonius CAD4 X-ray diffractometer using single crystals with graphite-monochromated Mo K $\alpha$  radiation ( $\lambda = 0.7107 \text{ \AA}$ ) by the  $\omega$ -scan method. The crystal data of the complex **3**·2DMF were collected on a Bruker-APEX-2 CCD X-ray diffractometer using single crystals with graphite-monochromated Mo K $\alpha$  radiation ( $\lambda = 0.7107 \text{ \AA}$ ) by the hemisphere method. Data were collected at 293 K. The coordinated DMF molecule is disordered and was refined over two sites with occupancies of 0.6 and 0.4, respectively. The refinement was performed using full-matrix least-squares with all non-hydrogen atoms refined anisotropically, except those belonging to the disordered coordinated DMF molecule, which were refined isotropically. The hydrogens were included on calculated positions, riding on their carrier atoms. The hydroxide O2–H hydrogen was found in the difference Fourier maps and refined with an O–H fixed distance of 0.90  $\text{\AA}$ . The crystal parameters and other experimental details of the data collections are summarized in Table 1.

Crystallographic data (excluding structure factors) have been deposited with the Cambridge Crystallographic Data Centre

(28) Otwinowski, Z.; Minor, Z. In *Methods Enzymol.*, Carter, C. W.; Sweet, R. M., Eds.; Academic Press: London, 1977; Vol. 276, Part A, pp 307–326.

(29) Blessing, R. H. *Acta Crystallogr., Sect. A* **1995**, *51*, 33–38.

(30) Altomare, A.; Burla, M. C.; Camalli, M.; Cascarano, G. L.; Giacovazzo, C.; Guagliardi, A.; Moliterni, A. G.; Polidori, G.; Spagna, R. *J. Appl. Crystallogr.* **1999**, *32*, 115–119.

(31) Sheldrick, G. M. *SHELXL97, Program for Crystal Structure Refinement*; University of Göttingen: Göttingen, Germany, 1997.

(32) Nardelli, M. *J. Appl. Crystallogr.* **1995**, *28*, 659–660.

(33) Farrugia, L. J. *J. Appl. Crystallogr.* **1999**, *32*, 837–838.

Table 1. Crystallographic Data for 1·0.5CH<sub>2</sub>Cl<sub>2</sub>, 2, and 3·2DMF

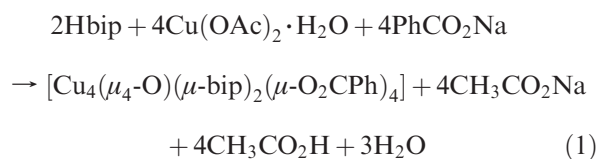
	1·0.5CH <sub>2</sub> Cl <sub>2</sub>	2	3·2DMF
formula	C <sub>74.5</sub> H <sub>63</sub> Cu <sub>4</sub> N <sub>4</sub> O <sub>11</sub> Cl	C <sub>46</sub> H <sub>42</sub> N <sub>16</sub> O <sub>4</sub> Cu <sub>4</sub>	C <sub>62</sub> H <sub>72</sub> N <sub>12</sub> O <sub>8</sub> S <sub>4</sub> Cu <sub>4</sub>
M g mol <sup>-1</sup>	1479.97	1137.13	1495.77
space group	<i>P</i> 2 <sub>1</sub> / <i>n</i>	<i>P</i> 2 <sub>1</sub> / <i>n</i>	<i>P</i> $\bar{1}$
cryst syst	monoclinic	monoclinic	triclinic
<i>a</i> /Å	13.7694(2)	8.571(3)	12.0338(6)
<i>b</i> /Å	23.8283(3)	24.548(5)	12.9150(7)
<i>c</i> /Å	20.3394(3)	12.048(3)	14.1274(8)
$\alpha$ /deg			65.2500(10)
$\beta$ /deg	97.0892(7)	109.52(7)	80.906(2)
$\gamma$ /deg			87.583(2)
<i>U</i> /Å <sup>3</sup>	6622.37(16)	2389.3(15)	1968.18(18)
<i>T</i> /K	120	293	293
<i>Z</i>	4	1	2
<i>D</i> <sub>c</sub> /g cm <sup>-3</sup>	1.484	1.581	1.385
<i>F</i> (000)	3036	1156	852
$\mu$ (Mo K $\alpha$ )/cm <sup>-1</sup>	13.73	18.18	12.34
measd reflns	63 571	4439	26 923
unique reflns	11 643	4145	8722
<i>R</i> <sub>int</sub>	0.0851	0.0647	0.0327
obsd reflns [ <i>I</i> ≥ 2 $\sigma$ ( <i>I</i> )]	9336	2334	5994
$\theta_{\min}$ – $\theta_{\max}$ /deg	1.90–25.00	1.98–24.97	1.61–27.50
<i>hkl</i> ranges	–16,16; –27,28; –24,24	–10,0; 0,29; –13,14	–14,15; –16,16; –18,18
<i>R</i> ( <i>F</i> <sup>2</sup> ) <sup><i>a</i></sup> (obsd reflns)	0.0751	0.0606	0.0498
<i>wR</i> ( <i>F</i> <sup>2</sup> ) <sup><i>a</i></sup> (all reflns)	0.1937	0.1581	0.1511
no. variables	844	316	458
goodness of fit	1.159	0.988	1.011
$\Delta\rho_{\max}$ ; $\Delta\rho_{\min}$ /e Å <sup>-3</sup>	1.46; –0.74	0.720; –0.769	1.057; –0.530

$$^a R = \sum(|F_o| - |F_c|)/\sum|F_o|. wR = [\sum w(|F_o| - |F_c|)^2/\sum w(F_o)^2]^{1/2}. w = 0.75/(\sigma^2(F_o) + 0.0010F_o^2).$$

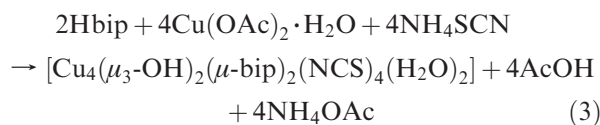
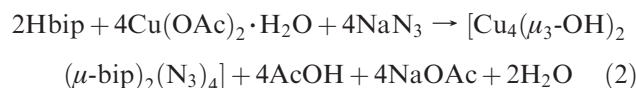
as supplementary publications CCDC-716090, -637273, and -744551. These data can be obtained free of charge at [www.ccdc.cam.ac.uk/conts/retrieving.html](http://www.ccdc.cam.ac.uk/conts/retrieving.html) [or from the Cambridge Crystallographic Data Centre, 12 Union Road, Cambridge CB2 1EZ, UK; fax: (internat.) +44-1223/336-033; e-mail: [deposit@ccdc.cam.ac.uk](mailto:deposit@ccdc.cam.ac.uk)].

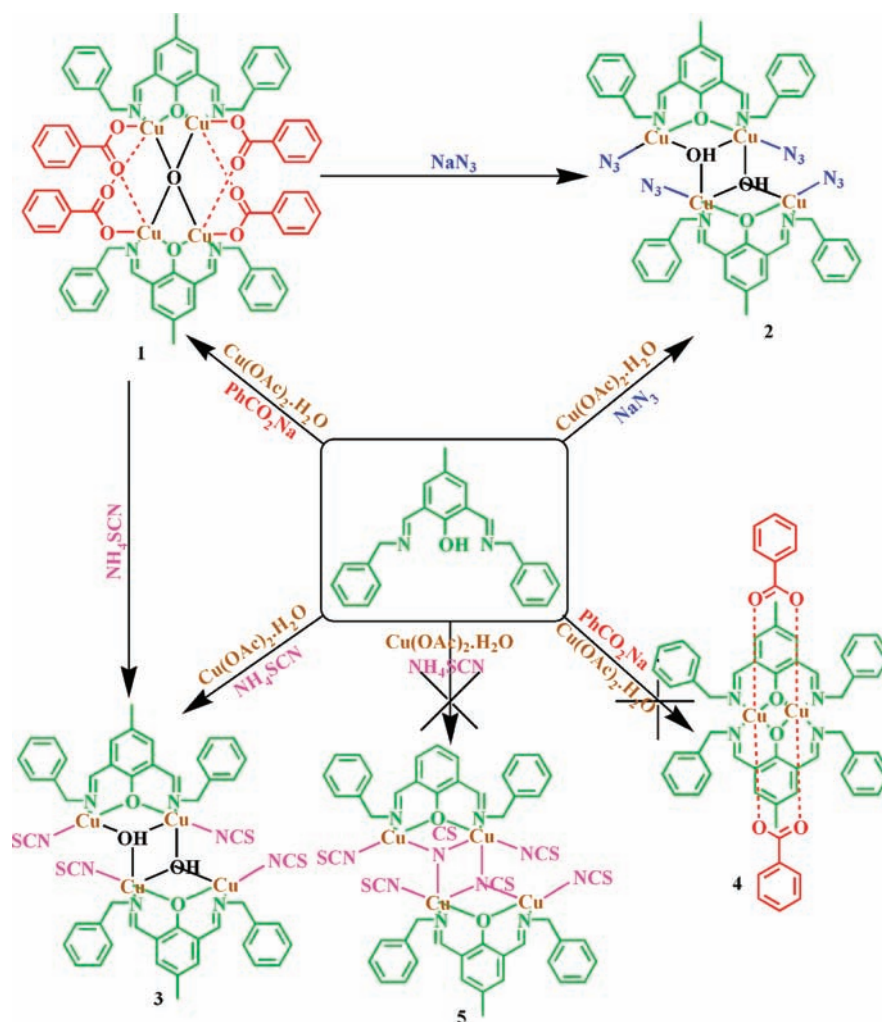
## Results and Discussion

**Synthetic Considerations.** The Schiff base 2,6-bis-(benzyliminomethyl)-4-methylphenol (Hbip) has been prepared (Scheme S1 in the Supporting Information) following a literature procedure,<sup>23</sup> and its reactions with copper(II) salts have been systematically investigated (Scheme 2). When the reaction of Cu(OAc)<sub>2</sub>·H<sub>2</sub>O was carried out with Hbip and PhCO<sub>2</sub>Na in MeOH and in the absence of base, [Cu<sub>4</sub>( $\mu_4$ -O)( $\mu$ -bip)<sub>2</sub>( $\mu$ -O<sub>2</sub>CPh)<sub>4</sub>] (**1**, Scheme 2) was obtained. In the absence of sodium benzoate, [Cu<sub>4</sub>( $\mu_4$ -O)( $\mu$ -bip)<sub>2</sub>( $\mu$ -OAc)<sub>4</sub>] was obtained as a green powder from the reaction mixture. At room temperature Cu(OAc)<sub>2</sub>·H<sub>2</sub>O, PhCO<sub>2</sub>Na, and Hbip in a 2:2:1 molar ratio have been mixed and stirred for 1 h to lead to complex **1**. The complex precipitates directly from the reaction mixture as a green solid in ~73% yield (note that several Cu/Hbip ratios were explored, but the 2:2:1 molar ratio gives the best yield and clean samples). The preparation of complex **1** is summarized in eq 1, accounting for the formation of the oxido bridge from the aqua molecule.



The elemental analysis and molar conductivity data are consistent with the formula [Cu<sub>4</sub>( $\mu_4$ -O)( $\mu$ -bip)<sub>2</sub>( $\mu$ -O<sub>2</sub>CPh)<sub>4</sub>] for **1**. However no sign of formation of only phenoxido-bridged Cu(II) dinuclear species (**4**, Scheme 2) was observed, perhaps because of the better stability of **1**, which crystallizes with a central tetrahedral  $\mu_4$ -oxido group to assemble a pair of [Cu<sub>2</sub>] units (it is worth noting that **4** was also not obtained when a MeOH solution of Hbip and PhCO<sub>2</sub>Na was added to Cu(OAc)<sub>2</sub>·H<sub>2</sub>O in a 1:2 molar ratio). Using a similar approach, two other reactions in the presence of azide and thiocyanate anions have been carried out. In these cases, the oxido bridge is converted in a hydroxido bridge. Green complexes [Cu<sub>4</sub>( $\mu_3$ -OH)<sub>2</sub>( $\mu$ -bip)<sub>2</sub>(N<sub>3</sub>)<sub>4</sub>] (**2**, Scheme 2) and [Cu<sub>4</sub>( $\mu_3$ -OH)<sub>2</sub>( $\mu$ -bip)<sub>2</sub>(NCS)<sub>4</sub>(H<sub>2</sub>O)<sub>2</sub>] (**3**, Scheme 2) are directly synthesized in ~70% yield from MeOH medium under aerobic conditions at room temperature by stirring a reaction mixture of Cu(OAc)<sub>2</sub>·H<sub>2</sub>O, Hbip, and NaN<sub>3</sub> or NH<sub>4</sub>SCN in a 2:1:2 molar ratio for 1 h. The same reactions in the presence of stoichiometric NEt<sub>3</sub> or NaOH gave the same products, confirming the formation of hydroxido bridges independently of the type and nature of added bases. The syntheses of **2** and **3** are summarized in eqs 2 and 3.

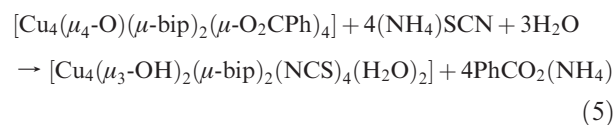
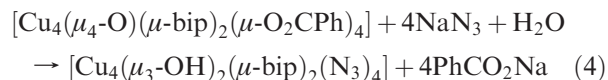


**Scheme 2.** Summary of the Possible Synthetic Routes That Lead to the Reported Complexes and Other Known Species for the Hbip Ligand

The elemental analysis and molar conductivity data confirm the respective formula. Reactions with an excess of azide or thiocyanate anions did not lead to the substitution of the hydroxido bridges in **2** and **3**, indicating the strong affinity and stability of the hydroxido bridges in these systems.

**Conversion of 1 to Stepped Cubane [Cu<sub>4</sub>] Complexes.** Green complexes [Cu<sub>4</sub>(μ<sub>3</sub>-OH)<sub>2</sub>(μ-bip)<sub>2</sub>(N<sub>3</sub>)<sub>4</sub>] (**2**) and [Cu<sub>4</sub>(μ<sub>3</sub>-OH)<sub>2</sub>(μ-bip)<sub>2</sub>(NCS)<sub>4</sub>(DMF)<sub>2</sub>] (**3**) can be obtained from [Cu<sub>4</sub>(μ<sub>4</sub>-O)(μ-bip)<sub>2</sub>(μ-O<sub>2</sub>CPh)<sub>4</sub>] (**1**) on reaction with sodium azide and ammonium thiocyanate salts. The treatment of CH<sub>2</sub>Cl<sub>2</sub>–MeOH (1:1) solutions of **1** by four equivalents of NaN<sub>3</sub> or NH<sub>4</sub>SCN readily leads to stepped cubane complex **2** or **3** with color changes from green to green followed by precipitation of green solids. The precipitates were filtered, washed with MeOH, dried, and dissolved in DMF for crystallization. Green crystals of **2** and **3** grow slowly over several days and can be isolated by filtration. Complexes **2** and **3** turn out to be novel examples of tetranuclear Cu<sup>II</sup> complexes in which the core of complex **1** is successfully modified by (i) replacing the benzoate bridges by N<sub>3</sub><sup>−</sup> and SCN<sup>−</sup> anions and (ii) converting (μ<sub>4</sub>-O) into (μ<sub>3</sub>-OH)<sub>2</sub> groups. The mechanism of the conversion of **1** to **2** and **3** summarized in eqs 4 and 5 is clearly complicated. It should be mentioned that the engaged O<sup>2−</sup> anion in **1** is a strong basic

group that reacts irreversibly with water to produce HO<sup>−</sup> anions trapped by **2** and **3** (eqs 4 and 5) in the same way as the reaction of K<sub>2</sub>O(s) with H<sub>2</sub>O (K<sub>2</sub>O + H<sub>2</sub>O → 2 KOH).<sup>34</sup>



These two reactions also demonstrate the successful replacement of the carboxylate groups with weak *apical*–*basal* bridging modes by strong azide and thiocyanate coordination groups on only the *basal* sites.

**IR Spectroscopy.** In the three [Cu<sub>4</sub>] complexes, the characteristic bands of the bip<sup>−</sup> ligand appear clearly on the FT-IR spectra. The ν<sub>C=N</sub> stretching frequencies are observed at 1623–1636 cm<sup>−1</sup> for complexes **1**–**3**. For **1**, the asymmetric and the symmetric stretching vibrations of the four bound carboxylate groups are detected at 1609 cm<sup>−1</sup>

(34) Myers, R. J. *J. Chem. Educ.* **1986**, *63*, 687–690.

as  $\tilde{\nu}_{\text{as}(\text{COO})}$ , while  $\tilde{\nu}_{\text{s}(\text{COO})}$  appeared at  $1371\text{ cm}^{-1}$  with a difference  $\Delta\tilde{\nu} = \tilde{\nu}_{\text{as}(\text{COO})} - \tilde{\nu}_{\text{s}(\text{COO})} = 238\text{ cm}^{-1}$ . This  $\Delta\tilde{\nu}$  value is in accord with the presence of  $\mu_{1,3}$ -carboxylato bridges between Cu(II) sites in **1** (it is worth noting that a nonbridging carboxylato group would lead to a larger  $\Delta\tilde{\nu}$  separation of ca.  $350\text{ cm}^{-1}$ ).<sup>35</sup> In the IR spectra of **1**, a sharp absorption band at  $623\text{ cm}^{-1}$  is detected. This band is missing from the IR spectra of the free Hbip ligand, sodium benzoate, and copper(II) acetate. This band is indeed associated with  $\tilde{\nu}_{\text{Cu-O}}$  frequencies originating from vibrations in the  $[\text{Cu}_4\text{O}]$  core in agreement with our recent report on  $[\text{Cu}_4(\mu_4\text{-O})(\text{bahped})_2](\text{ClO}_4)_2$ ,<sup>16</sup> which exhibits a  $[\text{Cu}_4\text{O}]$  band at  $566\text{ cm}^{-1}$ . In the case of  $[\text{Cu}_4\text{Cl}_4(\mu_4\text{-O})(\text{OSR}_2)_4]$  ( $\text{R} = \text{Et}, \text{}^n\text{Bu}$ )<sup>36</sup> and in copper 2,6-bis(morpholinomethyl)-4-methylphenol complexes,<sup>37</sup> this band is seen at  $581\text{--}592\text{ cm}^{-1}$ . As expected for complexes **2** and **3**·2DMF, the  $\tilde{\nu}_{\text{COO}}$  and  $\tilde{\nu}_{\text{Cu-O}}$  bands are missing and a broad band near  $3600\text{ cm}^{-1}$  is observed due to the  $\tilde{\nu}_{\text{OH}}$  stretching mode of the  $\text{HO}^-$  bridging groups.<sup>38</sup> In addition, complex **2** shows a very strong and sharp band at  $2043\text{ cm}^{-1}$  for the  $\tilde{\nu}_{\text{as}(\text{N-N-N})}$  asymmetric stretching vibration of the bound terminal  $\text{N}_3^-$  groups, while the symmetric vibration  $\tilde{\nu}_{\text{s}(\text{N-N-N})}$  appears as a weak band at  $1347\text{ cm}^{-1}$ .<sup>6</sup> The binding of thiocyanate anions in **3**·2DMF is clearly seen by the  $\tilde{\nu}_{\text{C-N}}$  stretching mode, which appears as a single intense band at  $2081\text{ cm}^{-1}$ .<sup>39</sup> The  $\tilde{\nu}_{\text{C-S}}$  stretching and the  $\delta_{\text{NCS}}$  bending frequencies in the  $800\text{--}400\text{ cm}^{-1}$  region could not be identified with certainty due to the presence of strong absorptions of the organic ligand in this region. The conversion of **1** to **2** or **3** in solution and in the solid state via a mechanochemical route (vide infra) has been well monitored using FT-IR spectroscopy and the characteristic bands of complexes **1**, **2**, and **3** (Figure 1).

**Electronic Spectra.** The three complexes in DMF solutions show multiple bands in the  $200\text{--}900\text{ nm}$  region. The ligand-field spectra of the complexes show broad absorption bands ( $\lambda$ ), with maxima at  $680$  ( $\epsilon = 210\text{ L mol}^{-1}\text{ cm}^{-1}$ ),  $655$  ( $\epsilon = 520\text{ L mol}^{-1}\text{ cm}^{-1}$ ), and  $665\text{ nm}$  ( $\epsilon = 525\text{ L mol}^{-1}\text{ cm}^{-1}$ ) for **1**, **2**, and **3**, respectively. The intense absorptions below  $400\text{ nm}$  at  $253\text{ nm}$  ( $\epsilon = 21695\text{ L mol}^{-1}\text{ cm}^{-1}$ ),  $274\text{ nm}$  ( $\epsilon = 13658\text{ L mol}^{-1}\text{ cm}^{-1}$ ), and  $274\text{ nm}$  ( $\epsilon = 13834\text{ L mol}^{-1}\text{ cm}^{-1}$ ) are dominated by the metal ion bound ligand-based absorptions for **1**·0.5 $\text{CH}_2\text{Cl}_2$ , **2**, and **3**·2DMF, respectively. Spectra of these complexes also record shoulders at  $389\text{ nm}$  ( $\epsilon = 4895\text{ L mol}^{-1}\text{ cm}^{-1}$ ),  $378\text{ nm}$  ( $\epsilon = 9480\text{ L mol}^{-1}\text{ cm}^{-1}$ ), and  $378\text{ nm}$  ( $\epsilon = 6820\text{ L mol}^{-1}\text{ cm}^{-1}$ ), respectively, due to  $\text{HO}^- \rightarrow \text{Cu}^{\text{II}}$  and  $\text{PhO}^- \rightarrow \text{Cu}^{\text{II}}$  ligand-to-metal charge transfer (LMCT) transitions.<sup>2</sup>

**Description of the Crystal Structures.**  $[\text{Cu}_4(\mu_4\text{-O})(\mu\text{-bip})_2(\mu\text{-O}_2\text{CPh})_4]\cdot 0.5\text{CH}_2\text{Cl}_2$  (**1**·0.5 $\text{CH}_2\text{Cl}_2$ ). The molecular structure of compound **1** is shown in Figure 2, and important bond lengths and angles are given in Table 2. Compound **1**·0.5 $\text{CH}_2\text{Cl}_2$  crystallizes in the monoclinic

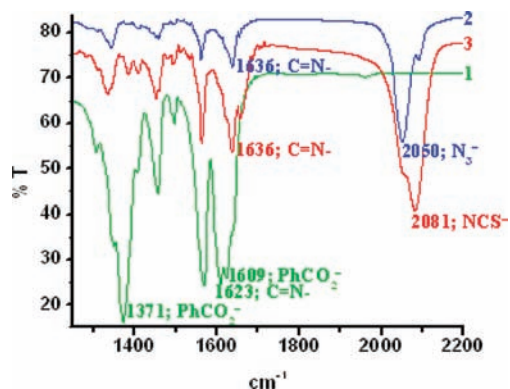


**Figure 1.** FT-IR spectra of **1**·0.5 $\text{CH}_2\text{Cl}_2$ , **2**, and **3**·2DMF between  $1250$  and  $2200\text{ cm}^{-1}$ .

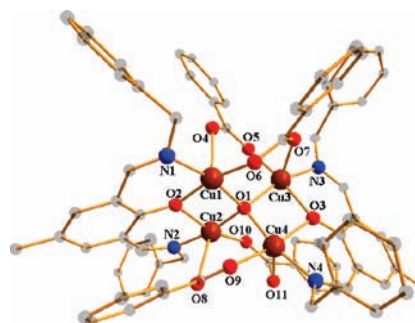


**Figure 2.** View of the molecular tetranuclear unit  $[\text{Cu}_4(\mu_4\text{-O})(\mu\text{-bip})_2(\mu\text{-O}_2\text{CPh})_4]$  in **1**·0.5 $\text{CH}_2\text{Cl}_2$  with atom-numbering scheme. H atoms are omitted for clarity. Color code:  $\text{Cu}^{\text{II}}$  brown, N blue, O red, C gray.

$P2_1/n$  space group. The asymmetric unit contains one tetranuclear complex and half of a dichloromethane molecule. The tetranuclear complex consists of two deprotonated  $\text{bip}^-$  ligands, each of them delivering a set of  $\text{N}_2\text{O}$  donor atoms to the  $[\text{Cu}_4]$  complex that assembles around a central  $\mu_4\text{-O}$  group. Four benzoate groups complete the coordination environments around each  $\text{Cu}^{\text{II}}$  site (Figures 2 and 3). The  $\text{O}^{2-}$  anion, O1, at the center of the complex is surrounded by four copper(II) ions organized in a distorted tetrahedral geometry with the  $\text{Cu}\cdots\text{Cu}$  distances varying from  $2.98$  to  $3.18\text{ \AA}$  (Figure S1, it should be noted that these  $\text{Cu}\cdots\text{Cu}$  distances are longer than those in the known benzoato-bridged copper paddlewheel dimers<sup>40</sup>). This  $\text{O}^{2-}$  oxygen anion thus provides a  $\mu_4$ -bridging connectivity to four  $\text{Cu}^{\text{II}}$ . The coordination sphere of each  $\text{Cu}^{\text{II}}$  adopts a distorted square-pyramid geometry due to the Jahn–Teller effect expected for  $3d^9$  copper(II) ion. The copper coordination sphere consists of two oxygen atoms from the carboxylato groups, one phenoxido oxygen and nitrogen atoms from the  $\text{bip}^-$  ligand, and one central  $\text{O}^{2-}$  anion (Figures S2 and S3). One of the carboxylato oxygen atoms is coordinating at the *apical* position of the  $\text{Cu}^{\text{II}}$  sites with bond distances of  $2.21\text{--}2.52\text{ \AA}$ , which are significantly longer, by  $0.2\text{--}0.3\text{ \AA}$ , than the other carboxylato oxygen atoms coordinated in  $\text{Cu}^{\text{II}}$  *basal* planes. The  $\text{Cu}\text{--}\text{O}_{\text{bz}}$  ( $\text{bz} = \text{benzoate}$ ) bond lengths in the *basal* plane ( $1.94\text{--}1.97\text{ \AA}$ ) are longer than the  $\text{Cu}\text{--}(\mu_4\text{-O})$  ( $1.91\text{--}1.93\text{ \AA}$ ) but close to the  $\text{Cu}\text{--}\text{O}_{\text{ph}}$  ( $1.97\text{--}2.00\text{ \AA}$ )

(35) Nakamoto, K. In *Infrared and Raman Spectra of Inorganic and Coordination Compounds, part B*; John Wiley & Sons: New York, 1997; pp 59–62; 276–282.

(36) Guy, J. T., Jr.; Cooper, J. C.; Gilardi, R. D.; Flippen-Anderson, J. L.; George, C. F., Jr. *Inorg. Chem.* **1988**, *27*, 635–638.

(37) Teipel, S.; Griesar, K.; Haase, W.; Krebs, B. *Inorg. Chem.* **1994**, *33*, 456–464.

(38) Motoda, K.-i.; Sakiyama, H.; Matsumoto, N.; Okawa, H.; Fentonb, D. E. *J. Chem. Soc., Dalton Trans.* **1995**, 3419–3425.

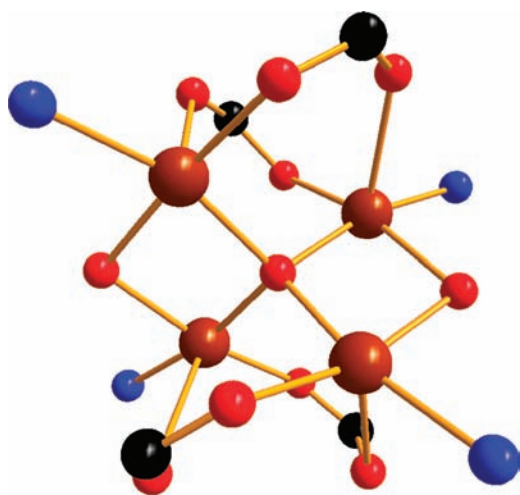
(39) Cortés, R.; Urriaga, M. K.; Lezama, L.; Pizarro, J. L.; Arriortua, M. I.; Rojo, T. *Inorg. Chem.* **1997**, *36*, 5016–5021.

(40) Takamizawa, S.; Miyake, R. *Chem. Commun.* **2009**, 4076–4078.

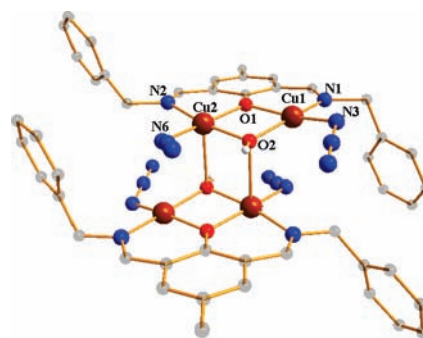
**Table 2.** Selected Interatomic Distances (Å) and Angles (deg) for  $1 \cdot 0.5 \text{CH}_2\text{Cl}_2$ 

Distances			
Cu1–O1	1.913(4)	Cu3–O1	1.932(4)
Cu1–O2	1.992(4)	Cu3–O3	2.003(4)
Cu1–O4	2.222(5)	Cu3–O5	1.945(4)
Cu1–O6	1.974(4)	Cu3–O7	2.214(5)
Cu1–N1	1.973(5)	Cu3–N3	2.000(5)
Cu2–O1	1.919(4)	Cu4–O1	1.916(4)
Cu2–O2	1.975(4)	Cu4–O3	1.976(4)
Cu2–O8	2.380(6)	Cu4–O9	1.963(5)
Cu2–O10	1.952(5)	Cu4–O11	2.522(6)
Cu2–N2	1.977(5)	Cu4–N4	1.971(5)
Cu1...Cu2	2.996(1)	Cu2...Cu3	3.309(1)
Cu1...Cu3	3.189(1)	Cu2...Cu4	3.146(1)
Cu1...Cu4	3.169(1)	Cu3...Cu4	2.986(1)

Angles			
O1–Cu1–O2	79.4(2)	O1–Cu3–O3	79.7(2)
O1–Cu1–O4	98.4(2)	O1–Cu3–O5	96.2(2)
O1–Cu1–O6	94.8(2)	O1–Cu3–O7	97.0(2)
O1–Cu1–N1	166.7(2)	O1–Cu3–N3	160.8(2)
O2–Cu1–O4	94.4(2)	O3–Cu3–O5	173.6(2)
O2–Cu1–O6	167.1(2)	O3–Cu3–O7	90.6(2)
O2–Cu1–N1	90.5(2)	O3–Cu3–N3	89.7(2)
O4–Cu1–O6	97.9(2)	O5–Cu3–O7	94.8(2)
O4–Cu1–N1	90.8(2)	O5–Cu3–N3	92.8(2)
O6–Cu1–N1	93.3(2)	O7–Cu3–N3	99.1(2)
O1–Cu2–O2	76.7(2)	O1–Cu4–O3	80.8(2)
O1–Cu2–O8	94.5(2)	O1–Cu4–O9	94.5(2)
O1–Cu2–O10	93.4(2)	O1–Cu4–O11	89.6(2)
O1–Cu2–N2	169.4(2)	O1–Cu4–N4	169.3(2)
O2–Cu2–O8	83.9(2)	O3–Cu4–O9	168.9(2)
O2–Cu2–O10	162.6(2)	O3–Cu4–O11	82.0(2)
O2–Cu2–N2	90.4(2)	O3–Cu4–N4	89.4(2)
O8–Cu2–O10	112.7(2)	O9–Cu4–O11	108.1(2)
O8–Cu2–N2	88.1(2)	O9–Cu4–N4	94.4(2)
O10–Cu2–N2	95.1(2)	O11–Cu4–N4	93.3(2)
Cu1–O1–Cu2	102.8(2)	Cu2–O1–Cu4	110.3(2)
Cu1–O1–Cu3	112.0(2)	Cu3–O1–Cu4	101.8(2)
Cu1–O1–Cu4	111.7(2)	Cu1–O2–Cu2	98.1(2)
Cu2–O1–Cu3	118.5(2)	Cu3–O3–Cu4	97.3(2)

**Figure 3.** View of the atom connectivity within the  $[\text{Cu}_4]$  tetrahedral core with the *basal*–*apical* carboxylate bridges in  $1 \cdot 0.5 \text{CH}_2\text{Cl}_2$ . Each carboxylate bridge joins the *basal* position of one copper atom with the *apical* position of another one. Color code:  $\text{Cu}^{\text{II}}$  brown, N blue, O red, C black.

bond lengths. A carboxylato bridge joins an *apical* binding site of one copper atom with a *basal* position of another copper atom (Figure S4). There are four such bridges of this type in the  $[\text{Cu}_4]$  molecule.

**Figure 4.** View of the molecular tetranuclear unit  $[\text{Cu}_4(\mu_3\text{-OH})_2(\mu\text{-bip})_2(\text{N}_3)_4]$  in **2** with atom-numbering scheme. H atoms are omitted for clarity. Color code:  $\text{Cu}^{\text{II}}$  brown, N blue, O red, C gray.

The  $\text{Cu}-\text{O}-\text{C}-\text{O}/\text{O}-\text{C}-\text{O}-\text{Cu}$  torsion angles ( $2.74^\circ/52.82^\circ$ ) indicate that copper atoms are bound by benzoates in a *syn*–*syn* (ideal values  $0^\circ/0^\circ$ ) arrangement, having out-of-plane binding for the second Cu atom. Within the  $[\text{Cu}_2(\mu\text{-bip})]^{3+}$  units, the bridging phenoxido oxygen atom shows a *basal*–*basal* coordination mode to two copper atoms. This mode of bridging allows the carboxylato oxygens to exhibit a complementary *basal*–*apical* coordination to  $\text{Cu}^{\text{II}}$  ions. This *basal*–*apical* and *apical*–*basal* combination is responsible for the formation of an interdimer cavity between  $[\text{Cu}_2(\mu\text{-bip})]^{3+}$  units that nicely traps the  $\text{O}^{2-}$  ion in **1**. The phenoxido oxygen bridge squeezes the  $\text{Cu}-(\mu_4\text{-O})-\text{Cu}$  ( $\text{Cu1}-\text{O1}-\text{Cu2}$  and  $\text{Cu3}-\text{O1}-\text{Cu4}$ ) angles to  $101.80^\circ$  compared to the other angles, at  $112.04^\circ$  ( $\text{Cu1}-\text{O1}-\text{Cu3}$  and  $\text{Cu2}-\text{O1}-\text{Cu4}$ ). Two phenoxido-bridged  $[\text{Cu}_2]$  fragments stay almost perpendicular to each other, with a dihedral angle of  $86.89^\circ$  between the two  $\text{Cu}_2\text{O}_2$  planes. All these distances and angles are in good agreement with previously reported values.<sup>37,41–44</sup> The four Cu atoms are placed approximately  $0.13$ – $0.19$  Å from their least-squares basal planes toward the apical carboxylato oxygen atoms. The coordination geometry about the metal ions is very close to square pyramidal (Addison parameter  $\tau$  varies from  $0.004$  to  $0.210$ ).<sup>45</sup> Within the crystal packing no H-bonding network or  $\text{CH}\cdots\pi$  interactions are present even in the presence of solvate  $\text{CH}_2\text{Cl}_2$  molecules within the lattice. The crystal-packing diagram along the *a* axis is shown in Figure S5 (see Supporting Information).

$[\text{Cu}_2(\mu_3\text{-OH})(\mu\text{-bip})(\text{N}_3)_2]_2$  (**2**). The molecular structure of  $[\text{Cu}_2(\mu_3\text{-OH})(\mu\text{-bip})(\text{N}_3)_2]_2$  is shown in Figure 4, and selected bond lengths and angles are listed in Table 3. The complex **2** crystallizes in the  $P2_1/n$  space group, and the asymmetric unit contains one-half of the tetranuclear unit (the second half of the tetramer is generated by the  $(-x, -y, 1-z)$  symmetry operator). The  $[\text{Cu}_4]$  complex results from the assembly of two  $[\text{Cu}_2(\mu\text{-OH})(\mu\text{-bip})(\text{N}_3)_2]$  fragments through two hydroxido groups ( $\text{O2}$  and  $\text{O2}^*$ ) that

(41) Mukherjee, S.; Weyhermüller, T.; Bothe, E.; Wieghardt, K.; Chaudhuri, P. *Eur. J. Inorg. Chem.* **2003**, 863–875.

(42) Chen, L.; Breeze, S.; Rousseau, R.; Wang, S.; Thompson, L. *Inorg. Chem.* **1995**, *34*, 454–465.

(43) Breeze, S. R.; Wang, S.; Chen, L. *J. Chem. Soc., Dalton Trans.* **1996**, 1341–1349.

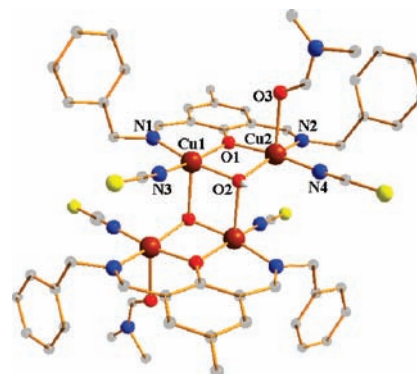
(44) Reim, J.; Griesar, K.; Haase, W.; Krebs, B. *J. Chem. Soc., Dalton Trans.* **1995**, 2649–2656.

(45) Addison, A. W.; Rao, T. N.; Reedijk, J.; van Rijn, J.; Verschoor, G. V. *J. Chem. Soc., Dalton Trans.* **1984**, 1349–1356.

**Table 3.** Selected Interatomic Distances (Å) and Angles (deg) for **2**

Distances			
N(3)–Cu(1)	1.972(6)	Cu(2)–N(2)	1.971(6)
Cu(2)–N(6)	1.933(7)	Cu(1)–O(2)	1.934(5)
Cu(2)–O(2)	1.962(4)	Cu(1)–N(1)	1.951(5)
Cu(2)–O(1)	1.963(4)	Cu(1)–O(1)	1.987(4)
Angles			
N(4)–N(3)–Cu(1)	119.4(5)	O(2)–Cu(1)–N(3)	96.0(2)
N(6)–Cu(2)–O(2)	95.3(2)	N(1)–Cu(1)–N(3)	96.5(2)
N(6)–Cu(2)–O(1)	169.8(3)	O(2)–Cu(1)–O(1)	76.90(18)
O(2)–Cu(2)–O(1)	76.82(18)	N(1)–Cu(1)–O(1)	92.47(19)
N(6)–Cu(2)–N(2)	95.2(3)	N(3)–Cu(1)–O(1)	165.2(2)
O(2)–Cu(2)–N(2)	169.2(2)	Cu(2)–O(1)–Cu(1)	101.88(18)
O(1)–Cu(2)–N(2)	92.5(2)	Cu(1)–O(2)–Cu(2)	103.9(2)
O(2)–Cu(1)–N(1)	165.6(2)	N(7)–N(6)–Cu(2)	121.5(7)

bridge pentacoordinated pyramidal Cu<sup>II</sup> ions (Cu2) in the apical directions (Figures S6–S10). The coordination sphere of Cu2 is very close to the perfect square-pyramidal geometry ( $\tau = 0.01$ ) induced by the Jahn–Teller effect, with significant elongation of the apical bonds by 0.4–0.5 Å (Cu2–O2\*, 2.491 Å). The in-plane Cu–O<sub>hy</sub> (hy = hydroxido) bond distances fall in the 1.926 to 1.958 Å range, which is comparable to those reported for other  $\mu$ -OH-bridged tetranuclear complexes.<sup>46,47</sup> On the other hand, Cu1 adopts a square-planar coordination sphere consisting of one O atom from a bridging hydroxido anion, one phenoxido O atom, one N atom from the imine group of the bip<sup>−</sup> ligand, and one N atom from an azido anion. In their square-pyramidal Cu2 and square-planar Cu1 coordination sphere, the Cu ions are displaced by 0.07 and 0.03 Å, respectively, from the O<sub>2</sub>N<sub>2</sub> mean basal planes. The C=N and C–O distances of the dialdimine and phenoxide fragments are consistent with the coordination of these functionalities.<sup>48,49</sup> The tetranuclear [Cu<sub>2</sub>( $\mu_3$ -OH)( $\mu$ -bip)(N<sub>3</sub>)<sub>2</sub>]<sub>2</sub> complex is centrosymmetric with a stepped cubane or ladder-type geometry (Figure S7) that results from the stacking of [Cu<sub>2</sub>O<sub>2</sub>] dinuclear cores (O are phenoxido and hydroxido oxygen atoms). Within this phenoxido–hydroxido-bridged [Cu<sub>2</sub>( $\mu$ -OH)( $\mu$ -bip)(N<sub>3</sub>)<sub>2</sub>] fragment, the Cu ions are separated by 3.06 Å. The Cu···Cu distance (3.31 Å) is longer for the bis-hydroxido-bridged Cu motif, which implies *apical* positions. As already mentioned above, the O2 and O2\* atoms of HO<sup>−</sup> anions act as  $\mu_3$  bridges forming two equally short bonds to Cu1 and Cu2 atoms, while the Cu–O bond to a third copper (Cu2\*) atom is longer by 0.53 Å. Hydrogen atom positions as well as the temperature displacement parameters on the hydroxido groups were refined without any restraints, indicating that the oxygen atoms O2 and O2\* are protonated. A monodentate azide anion is coordinated to each copper site. The azido terminal groups are both almost linear, with an N–N–N angle of  $\sim 175^\circ$ , but they

**Figure 5.** View of the molecular tetranuclear unit [Cu<sub>4</sub>( $\mu_3$ -OH)<sub>2</sub>( $\mu$ -bip)<sub>2</sub>-(NCS)<sub>4</sub>(DMF)<sub>2</sub>] in **3**·2DMF with atom-numbering scheme. H atoms are omitted for clarity. Color code: Cu<sup>II</sup> brown, N blue, O red, S yellow, C gray.**Table 4.** Selected Interatomic Distances (Å) and Angles (deg) for **3**·2DMF

Distances			
Cu(1)–O(2)	1.924(2)	Cu(2)–O(2)	1.927(2)
Cu(1)–N(3)	1.949(3)	Cu(2)–N(4)	1.940(3)
Cu(1)–N(1)	1.965(3)	Cu(2)–N(2)	1.972(3)
Cu(1)–O(1)	1.978(2)	Cu(2)–O(1)	1.975(2)
Cu(1)–O(2) <sup>a</sup>	2.331(2)	Cu(2)–O(3)	2.337(6)
Cu(1)–Cu(2)	3.0425(6)	O(2)–Cu(1) <sup>a</sup>	2.331(2)

Angles			
O(2)–Cu(1)–N(3)	94.82(12)	O(2)–Cu(2)–N(2)	159.44(11)
O(2)–Cu(1)–N(1)	167.72(11)	N(4)–Cu(2)–N2	97.08(13)
N(3)–Cu(1)–N(1)	96.65(13)	O(2)–Cu(2)–O(1)	76.69(9)
O(2)–Cu(1)–O(1)	76.70(9)	N(4)–Cu(2)–O(1)	170.31(12)
N(3)–Cu(1)–O(1)	163.66(13)	N(2)–Cu(2)–O(1)	92.00(11)
N(1)–Cu(1)–O(1)	91.11(11)	O(2)–Cu(2)–O(3)	103.14(16)
O(2)–Cu(1)–O(2) <sup>a</sup>	84.90(9)	N(4)–Cu(2)–O(3)	90.30(19)
N(3)–Cu(1)–O(2) <sup>a</sup>	98.51(12)	N(2)–Cu(2)–O(3)	94.32(16)
N(1)–Cu(1)–O(2) <sup>a</sup>	97.69(11)	O(1)–Cu(2)–O(3)	92.35(16)
O(1)–Cu(1)–O(2) <sup>a</sup>	94.66(9)	C(24)–N(3)–Cu(1)	169.5(4)
O(2)–Cu(2)–N(4)	93.64(12)	C(25)–N(4)–Cu(2)	169.0(4)

<sup>a</sup> =  $-x, -y, 2-z$ .

show a nonlinear monodentate binding mode on the Cu(II) ions, having an average Cu–N–N angle of  $\sim 120^\circ$  and Cu–N separations of 1.93–1.97 Å. These Cu–N bond distances are short in comparison to the *basal*–*apical* bridging azides (1.98 and 2.33 Å).<sup>10</sup> It is interesting to note that the two outer copper ions (Cu1 and Cu1\*) show intermolecular Cu···N<sub>az</sub> contacts at a distance of 2.79 Å (Figures S11 and S12), while intramolecular Cu···N<sub>az</sub> separations are around 2.87 Å. These intercomplex interactions are operative via a  $\mu$ -1,1-bridging coordination mode of the azide anion (with a Cu–N<sub>az</sub>–Cu angle of 98.99°, similar to the other azide-bridged Cu<sup>II</sup> complexes<sup>50</sup>) and lead to a one-dimensional assembly of tetranuclear [Cu<sub>2</sub>( $\mu_3$ -OH)( $\mu$ -bip)(N<sub>3</sub>)<sub>2</sub>]<sub>2</sub> complexes.

[Cu<sub>4</sub>( $\mu_3$ -OH)<sub>2</sub>( $\mu$ -bip)<sub>2</sub>(NCS)<sub>4</sub>(DMF)<sub>2</sub>] (**3**·2DMF). Compound **3** crystallizes in triclinic space group *P* $\bar{1}$  with an inversion center at the midpoint of Cu2···Cu2\*. The molecular structure of **3** is shown in Figure 5, and the relevant metric parameters are collected in Table 4. The molecular structures of **2** and **3** are essentially the same

(46) Graham, B.; Hearn, M. T. W.; Junk, P. C.; Kepert, C. M.; Mabbs, F. E.; Moubarak, B.; Murray, K. S.; Spiccia, L. *Inorg. Chem.* **2001**, *40*, 1536–1543.

(47) Alzuet, G.; Real, J. A.; Borrás, J.; Santiago-García, R.; García-Granda, S. *Inorg. Chem.* **2001**, *40*, 2420–2423.

(48) Mukhopadhyay, U.; Govindasamy, L.; Ravikumar, K.; Velmurugan, D.; Ray, D. *Inorg. Chem. Commun.* **1998**, *1*, 152–154.

(49) Fondo, M.; García-Deibe, A. M.; Bermejo, M. R.; Sanmartín, J.; Llamas-Saiz, A. L. *J. Chem. Soc., Dalton Trans.* **2002**, 4746–4750.

(50) Mondal, K. C.; Mukherjee, P. S. *Inorg. Chem.* **2008**, *47*, 4215–4225.



with the exception that all  $\text{Cu}^{\text{II}}$  metal ions are pentacoordinated with square-pyramid geometry in **3** owing to the Jahn–Teller effect, with significant elongation of the apical bonds by 0.20–0.30 Å. Compound **3** differs also from **2** due to the presence of terminal  $\text{NCS}^-$  groups (instead of  $\text{N}_3^-$  anions in **2**) and DMF molecules present in the crystal packing and also on the apical position of the Cu2 site. These differences induce only slight geometrical changes, while the overall structure of the complex is preserved (Figure S13). The equatorial positions of both copper sites, Cu1 and Cu2, are occupied by the imine N1 (for Cu1) or N2 (for Cu2) and phenoxido O1 atoms from the  $\text{bip}^-$  ligand, a hydroxido O2 group, and N3 (for Cu1) or N4 (for Cu2) from  $\text{NCS}^-$  anions. The  $\text{N}_{\text{im}}-\text{Cu}-\text{N}_{\text{th}}$  (th = thiocyanate) and  $\text{N}_{\text{im}}-\text{Cu}-\text{O}_{\text{ph}}$  bite angles average  $96.86^\circ$  and  $92.76^\circ$ , respectively. The  $\text{Cu}-\text{O}_{\text{hy}}$  basal distances fall in the 1.924–1.927 Å range, which is comparable to bond distances reported for other  $\mu$ -hydroxido-bridged tetranuclear complexes.<sup>46,47</sup>

The apical positions of the pentacoordinated Cu1 and Cu2 metal ions are occupied by hydroxido O2\* and DMF oxygen, O3, atoms at  $\text{Cu}-\text{O}$  distances of 2.332 and 2.337 Å, respectively. The Cu(II) metal ions are displaced by 0.14 and 0.16 Å, respectively, from the  $\text{O}_2\text{N}_2$  mean basal planes. The  $\text{Cu}-\text{O}_{\text{hy}}$  apical distance (2.33 Å) is significantly shorter in **3** than in **2** (2.49 Å). The phenoxido- and hydroxido-bridged Cu atoms ( $\text{Cu1}\cdots\text{Cu2}$ ) are separated by 3.04 Å with  $\text{Cu}-\text{O}-\text{Cu}$  angles of  $104.38^\circ$  and  $100.65^\circ$ , whereas bis-hydroxido-bridged Cu atoms ( $\text{Cu2}\cdots\text{Cu2}^*$ ) show a longer  $\text{Cu}\cdots\text{Cu}$  distance of 3.15 Å with a  $\text{Cu}-\text{O}-\text{Cu}$  angle of  $95.08^\circ$ . In **3**, a thiocyanate anion is coordinating each Cu site in a quasi-linear fashion with an average  $\text{Cu}-\text{N}_{\text{th}}-\text{C}$  angle of  $\sim 169.23^\circ$  and  $\text{Cu}-\text{N}_{\text{th}}$  separations of 1.940–1.950 Å. The thiocyanato groups are themselves almost linear, with an average  $\text{N}-\text{C}-\text{S}$  angle of  $\sim 178^\circ$ . Unlike compound **2**, the presence of a DMF solvent molecule in the apical position of the outer copper ions, Cu2, prevents any kind of short intermolecular  $\text{Cu}\cdots\text{S}_{\text{th}}$  contacts between neighboring molecules (Figure S14). Nevertheless, two intermolecular hydrogen bonds are observed with  $\text{O}\cdots\text{O}$  distances of 2.745 Å between oxygen atoms of interstitial DMF molecules and the hydrogen atoms of hydroxido groups (Figure S15).

**Role of  $\text{PhCO}_2^-$  and  $\text{N}_3^-$  or  $\text{NCS}^-$  Anions for Different Molecular Assemblies.** The well-established  $\mu_{1,3}$  bridging mode of  $\text{PhCO}_2^-$  groups helps the trapping of the oxido group within the  $[\text{Cu}_4\text{O}]$  tetrahedron in **1** by maintaining the required  $\text{Cu}\cdots\text{Cu}$  separation to attract a  $\mu_4\text{-O}$  atom. In the case of **2** and **3**, a  $\mu_{1,3}$  bridging mode is not possible for either  $\text{N}_3^-$  or  $\text{NCS}^-$ . As a result, the reaction of **1** with  $\text{N}_3^-$  or  $\text{NCS}^-$  substitutes all carboxylate groups and converts the  $\mu_4$ -oxido core into a bis-hydroxido core with the binding of the pseudo-halide ions in monodentate fashions. The  $\text{N}_3^-$  or  $\text{NCS}^-$  anions replace efficiently the benzoate groups and cleave the tetrahedron  $[\text{Cu}_4\text{O}]$  core into two phenoxido-bridged  $[\text{Cu}_2]$  fragments, which ultimately reassemble around two hydroxido groups.

**Binding of  $\text{N}_3^-$  and  $\text{NCS}^-$  in  $[\text{Cu}_4]$  Stepped Cubane Complexes.** The binding of  $\text{N}_3^-$  and  $\text{NCS}^-$  anions to the  $\text{Cu}^{\text{II}}$  centers of complex **1** in 1:1 fashion that yields new neutral complexes **2** and **3** is reminiscent of the  $\text{N}_2\text{O}$  binding via N in  $\text{Cu}^{\text{II}}$ -based nitrous oxide reductase. The bridging benzoate anions originally present in **1** are

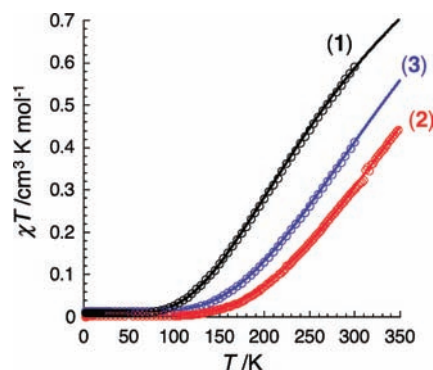


**Figure 6.** Temperature dependence of  $\chi T$  product ( $\chi$  being the molar magnetic susceptibility defined as  $M/H$ ) for **1**·0.5 $\text{CH}_2\text{Cl}_2$  (in black), **2** (in red), and **3**·2DMF (in blue) at 1000 Oe. The solid lines are the best fits obtained using the isotropic Heisenberg model described in the text with two isolated dinuclear  $S = 1/2$  units.

substituted during the reaction by  $\text{N}_3^-$  and  $\text{NCS}^-$  groups, which coordinate in a monodentate fashion the Cu sites by the N ends of these incoming groups. During this substitution the  $\mu_4\text{-O}$  central atom of **1** is converted to two  $\text{HO}^-$  bridges most probably from the attack of solvent water molecules or moisture from the air (eq 4). The irreversible conversions of **1** to **2** and **3** are due to a better coordination ability of pseudo-halide anions in monodentate mode compared to the *syn-syn basal-apical* bridging mode of the benzoate groups. Thus these two  $\text{N}_3^-$  and  $\text{NCS}^-$  groups replace benzoates spontaneously. Replacement of the four benzoates by the same numbers of  $\text{N}_3^-$  or  $\text{NCS}^-$  anions retains the electroneutrality of the resulting complexes with concomitant oxido to bis-hydroxido bridge conversion.

**Water-Assisted Mechanochemical Core Conversions.** Intimate mixing and grinding of **1** with  $\text{NaN}_3$  or  $\text{NH}_4\text{SCN}$  in an agate mortar (as normally done for preparing samples for IR spectroscopy) and thorough washing with water (that removes sodium benzoate from the products) led to the quantitative transformations to **2** and **3**, as identified by FTIR measurement, solubility differences, and determinations of unit cells of grown single crystals from powder samples (the resulting IR spectra and cell parameters are given in the Supporting Information). This synthetic mechanochemical method is an interesting alternative process to the traditional one performed in solution. It allows a rapid test of possible complex core conversions in a given metal–ligand system. In the present case, this approach is useful to study the stability of a  $[\text{Cu}_4]$  stepped cubane compound without the presence of multiple species in equilibrium in traditional solution-based syntheses. The PXRD data have been taken to identify the phase change from **1** to **2** or **3** core conversions. The PXRD patterns of the three complexes are shown in Figure S17 (Supporting Information). These patterns are consistent with those of simulated ones obtained from the single-crystal X-ray diffraction data.

**Magnetic Properties.** The solid-state magnetic properties of **1**·0.5 $\text{CH}_2\text{Cl}_2$ , **2**, and **3**·2DMF have been investigated by dc susceptibility measurements down to 1.8 K at 0.1 T (Figure 6). At room temperature, the  $\chi T$  products are  $0.59 \text{ cm}^3 \text{ K mol}^{-1}$ ,  $0.29 \text{ cm}^3 \text{ K mol}^{-1}$ , and  $0.41 \text{ cm}^3 \text{ K mol}^{-1}$  for **1**, **2**, and **3**, respectively. The values of

$\chi T$  are far from the theoretical value of  $1.5 \text{ cm}^3 \text{ K mol}^{-1}$  (with  $g = 2$ ) expected for four isolated paramagnetic  $\text{Cu}^{\text{II}}$  ions ( $d^9$ ,  $S = 1/2$ ), indicating strong and dominant antiferromagnetic interactions between the  $\text{Cu}^{\text{II}}$  ions in the three compounds. Upon cooling, both  $\chi T$  products continuously decrease to reach a value close to zero below 70, 120, and 100 K, for **1**, **2**, and **3**, respectively (Figure 6), as expected when intracomplex antiferromagnetic interactions induce a singlet spin ground state.

Generally speaking for the  $\text{Cu}^{\text{II}}$  ions, the magnetic interactions mediated through their *apical* positions are much weaker than those mediated by bridges coordinated on the *equatorial* sites. Therefore, if one considers only the magnetic pathways that involve equatorial bonds around each  $\text{Cu}^{\text{II}}$  ion, the complexes **2** and **3** can be viewed as two almost isolated  $\text{Cu1-Cu2}$  dinuclear units with a double phenoxido-hydroxido bridge (Figures 4 and 5). For **1**, the situation is slightly different due to the presence of the central  $\mu_4$ -oxido bridge between  $\text{Cu(II)}$  ions. Nevertheless, the magnetic pathway through the double  $\mu_4$ -oxido/phenoxido bridges is likely much more efficient than a single  $\mu_4$ -oxido bridge between two  $\text{Cu(II)}$  metal ions. As a consequence, the magnetic description of **1** is similar to **2** and **3** (vide supra) with two isolated  $\text{Cu1-Cu2}$  and  $\text{Cu3-Cu4}$  dinuclear units with a double phenoxido-oxido bridge (Figures 2 and 3). Moreover, considering the similarity of the bridging modes in the two dinuclear  $\text{Cu1-Cu2}$  and  $\text{Cu3-Cu4}$  units in **1** (Table 2), the interaction in the two spin dimers is expected to be similar. Considering these magnetostructural remarks, the magnetic properties of the three compounds can be analyzed in a first approximation with the same magnetic model including two identical  $S = 1/2$  spin dimers with only one exchange parameter, noted  $J$ . The magnetic susceptibility has been thus calculated from the following isotropic spin Heisenberg Hamiltonian:

$$H = -2J\{S_{\text{Cu},1} \cdot S_{\text{Cu},2}\}$$

where  $S_i$  are the spin operators for each center with  $S = 1/2$ . The application of the van Vleck equation<sup>51,52</sup> allows the determination of the low-field analytical expression of the magnetic susceptibility<sup>53</sup> taking into account the presence of residual paramagnetic contribution:

$$\chi T = 2(1 - \rho) \frac{2N\mu_{\text{B}}^2 g_{\text{Cu}}^2}{k_{\text{B}}} \frac{1}{3 + e^{-2J/k_{\text{B}}T}} + \rho \frac{N\mu_{\text{B}}^2 g_{\text{Cu}}^2}{2k_{\text{B}}}$$

As shown in Figure 6, the above expression of the magnetic susceptibility reproduces almost perfectly the experimental data at 1000 Oe. The best sets of parameters obtained are given in Table 5 for the three compounds. The negative sign of the magnetic interactions implies that these  $\text{Cu}^{\text{II}}$  dimer units and thus the tetranuclear complexes possess an  $S_{\text{T}} = 0$  spin ground state, i.e., diamagnetic ground state. The  $\rho$  values indicate that a very small amount of residual paramagnetic contribution is present in the measured samples of **1** and **3**, as often

**Table 5.** Parameters Deduced from the Analysis of the Magnetic Properties for **1**, **2**, and **3**

	$g$	$J/k_{\text{B}}$ (K)	$\rho$ (%)
<b>1</b>	2.0(1)	-289(4)	2
<b>2</b>	2.2(1)	-464(5)	0
<b>3</b>	2.2(1)	-405(15)	2

seen for materials displaying a diamagnetic ground state. Taking into account that the impurity possesses a Curie paramagnetic behavior and the same molecular weight as the major complex, the amount is about 2% for **1** and **3**.

It is worth mentioning that for **1** the magnetic properties have also been analyzed with an alternative model including two different intramolecular interactions, one mediated by the double oxido/phenoxido bridges and the other one mediated by single  $\mu_4$ -oxido bridges.<sup>54</sup> Indeed as soon as two interactions are considered in the model, more than one set of parameters can reproduce well the experimental data, suggesting an overparametrization in the fitting procedure. Therefore the only relevant model requires no more than one interaction parameter, as shown in Figure 6, and thus it is not possible to evaluate the magnetic interaction through the single  $\mu_4$ -oxido bridge. The amplitude of the antiferromagnetic exchange parameter is relatively large for the three compounds but stays in the range of magnitude observed in similar compounds with same type of double oxido-phenoxido bridges.<sup>54,55</sup> These results confirm the efficiency of this type of double oxido-phenoxido or hydroxido-phenoxido bridge to mediate strong antiferromagnetic couplings.

## Conclusions

The coordination chemistry of the  $\text{bip}^-$  phenolate-centered ligand in presence of  $\text{Cu(II)}$  metal ions has been studied in this work and confirms the key role of ancillary and nucleating groups in the synthesis of new  $[\text{Cu}_4]$  assemblies. The type of bridging co-ligands ( $\text{O}^{2-}$  or  $\text{HO}^-$ ) seems to dictate the final topologies for the resulting complexes. Three tetranuclear copper complexes were investigated by X-ray diffraction on single crystals and magnetic susceptibility measurements. The dinucleating ligand  $\text{bip}^-$  facilitates the assembly of two  $\text{Cu}^{\text{II}}$  pairs in two different topologies, e.g., tetrahedral and stepped cubanes, leaving three coordinating sites open per metal for binding exogenous ligands. The binding of ancillary ligands such as  $\text{N}_3^-$  and  $\text{NCS}^-$  induces the conversion of the tetrahedral  $[\text{Cu}_4(\mu_4\text{-O})]$  core observed in **1** into stepped cubane  $[\text{Cu}_4(\mu_3\text{-OH})_2]$  units in **2** and **3**. Our current work is dedicated to the use of different external bridges such as sulfide, peroxide, and bisulfide in this reaction system to induce the formation of other types of homo- and heterometallic complexes.

**Acknowledgment.** M.S. is thankful to the Council of Scientific and Industrial Research, New Delhi, for the

(51) van Vleck, J. H. *The Theory of Electric and Magnetic Susceptibility*; Oxford University Press, 1932.

(52) Kambe, K. *J. Phys. Soc. Jpn.* **1950**, *5*, 48–51.

(53) O'Connor, C. J. *Prog. Inorg. Chem.* **1982**, *29*, 203–283.

(54) Hall, J. W.; Estes, W. E.; Estes, E. D.; Scaringe, R. P.; Hatfield, W. E. *Inorg. Chem.* **1977**, *16*, 1572–1574.

(55) Adams, A.; Fenton, D. E.; Haque, S. R.; Heath, S.; Ohba, M.; Okawa, H.; Spey, S. E. *Dalton Trans.* **2000**, 1849–1856.

(56) Banerjee, A.; Sarkar, S.; Chopra, D.; Colacio, E.; Krishna, K. R. *Inorg. Chem.* **2008**, *47*, 4023–4031.

financial support. V.B. acknowledges Italian Ministry of University and Scientific Research (MIUR, Rome). R.C., C.M., and N.H. thank MAGMANet (Grant NMP3-CT-2005-515767), the Conseil Régional d'Aquitaine, GIS Advanced Materials in Aquitaine (COMET Project), the Université de Bordeaux, the CNRS, and the Natural

Science and Engineering Council (NSERC) of Canada for a year of postdoctoral fellowship.

**Supporting Information Available:** X-ray crystallographic file in CIF format, Schemes S1 to S2, Figures S1 to S17, and synthesis and characterization of ligand Hbip. This material is available free of charge via the Internet at <http://pubs.acs.org>.